Article

Strategy of Stem Cell Transplantation for Bone Regeneration with Functionalized Biomaterials and Vascularized Tissues in Immunocompetent Mice

He Zhang,[§] Xiaoming Fu,[§] Siqi Zhang, Qian Li, Yang Chen, Hao Liu, Wen Zhou, and Shicheng Wei*

Read Online

ACCESS | Metrics & More | Article Recommendations

ABSTRACT: The use of human bone marrow mesenchymal stem cells (hBMSCs) to regenerate and repair bone tissue defects is a complex research field of bone tissue engineering; nevertheless, it is a hot topic. One of the biggest problems is the limited survival and osteogenic capacity of the transplanted cells within the host tissue. Even for hBMSCs with their low immunogenicity, the body will still cause a local immune-inflammatory response directed against the allogeneic cells and thereby reduce the activity of the transplanted cells. Even in the case of successful transplantation, the lack of vascularization at the transplantation site makes it difficult for the transplanted cells to exchange nutrients and metabolic wastes that ultimately affects bone regeneration. In this study, we covalently modified alginate with RGD and QK peptides that were injected subcutaneously into immunocompetent mice. Histological analysis, as well as ELISA techniques, proved that this method is able to provide bioactive stem cell transplant beds containing functionalized biomaterials and vascularized surrounding tissues. Inflammation-related factors, such as IL-2, IL-6, TNF-α, and IFN-γ, around the cell graft beds decreased with time and were lowest at the second week. Then, the hBMSCs were injected into the cell transplantation beds intended to form vascularized bonelike tissues that were evaluated by micro-computed tomography (Micro CT), histological, and immunohistochemical analyses. The results showed that the expression of osteogenesis-related proteins RUNX2, COL1A1, and OPN, as well as the expression of angiogenic factor vWF and cartilage-related protein COL2A1 were significantly upregulated in the hBMSC-derived osteogenic tissue. These results suggest that the stem cell transplantation strategy by constructing bioactive cell transplant beds is effective to enhance the bone regeneration capacity of hBMSCs and holds great potential in bone tissue engineering.

KEYWORDS: vascularized bonelike tissues, bioactive stem cell transplantation beds, functionalized sodium alginate hydrogel, human bone marrow mesenchymal stem cells
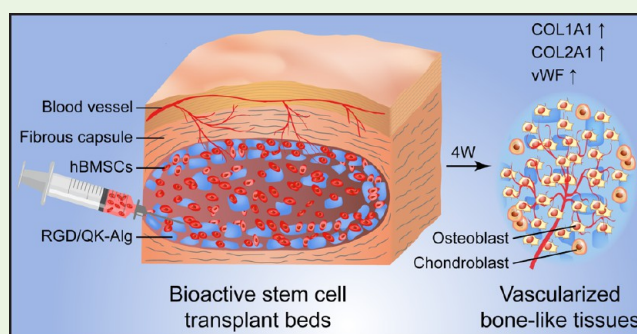
1. INTRODUCTION

Bone is a functional organ capable of limited self-healing and regeneration. Larger bone defects caused by trauma, congenital malformations, or tumor resection exceed the repair capacity of the bone tissue and do not heal without intervention, which seriously decreases the quality of life of the patient and imposes a heavy economic burden on society. Thus, the repair of large bone defects remains a prevalent and challenging problem.[1−4] Large bone defects are characterized by limited regenerative capacity and insufficient blood supply.[5−7] For the treatment of these defects, commonly bone grafts are used,[8] such as large segments of bone autografts[9,10] or bone constructs prepared from biomaterials.[11−14] To overcome the limited source of autologous bone grafts and donor site morbidity, many efforts have been made to identify bone substitutes.[15] One of the efforts comprises biological composites with osteogenesis inducing activity that bind to various active factors, such as those of the BMP family and vascular endothelial growth factor (VEGF), to promote the regenerative capacity of bone tissue defects.[16] However, the insufficient blood supply of the bone constructs is one of the key issues affecting bone tissue regeneration and repair.[17] The current common method of addressing blood supply deficiency is the application of VEGF to induce angiogenesis.[18] Unfortunately, VEGF cannot be used on a broader clinical basis due to its high cost and immunogenicity.[19,20] One

solution to this problem could be the recently emerged QK peptide, which mimics the function of VEGF. The QK peptide binds to and activates VEGF receptors to promote adhesion and proliferation of vascular endothelial cells[21,22] and has the advantages of low cost, easy synthesis, low immunogenicity, and better stability.[23−25]

Stem cell transplantation is the most promising research approach for the treatment of bone defects. For this, stem cells with osteogenic properties are transplanted into the bone defect area where they proliferate and differentiate into osteoblasts within the planting beds, so as to achieve bone regeneration and repair. Human bone marrow mesenchymal stem cells (hBMSCs) are the most commonly used seed cells because of their abundance, easy isolation, in vitro cultivation technique, strong self-renewal ability, and finally their multi-directional differentiation potential.[26] However, direct cell transplantation into a bone defect site often fails, resulting in the loss of most of the cells.[27,28] Additionally, even for hBMSCs with their low immunogenicity, the body's immune rejection or foreign body response to allogeneic cells cannot be circumvented, which further affects cellular activity and osteogenesis.[29,30] The problem is even more pronounced in larger bone defects due to the need of higher cell numbers and their decreased ability of regeneration and repair. Liu and Jin have shown that biomimetic hierarchical intrafibrillarly mineralized collagen facilitated M2 macrophage polarization and interleukin-4 secretion to promote MSC osteogenic differentiation.[31] However, exogenous MSCs lack the adaptive processes used in vivo to enhance their activity and osteogenic capacity. Sodium alginate is a biocompatible and injectable material that has been widely used in bone tissue engineering, whereas RGD peptide is one of the most widely used peptides in biomaterial modification approaches. Its cell binding sequence "Arg-Gly-Asp" is recognized by integrin receptors on the cell surface to promote cell adhesion, proliferation, and differentiation.[29,32,33] Wei and Luo have shown that the combination of RGD-modified gels or three-dimensional (3D) porous scaffolds as carriers of hBMSCs for in vivo trans-plantation purposes can improve their proliferation and differentiation ability and therefore contribute to the repair of damaged bone tissue.[34−37] However, the problem of immunological rejection caused by allogenic cell trans-plantation remains unresolved. Andrew implanted an inert biomaterial silicone rubber tube subcutaneously into mice to purposely induce a foreign body reaction and thereby generate a fibrous capsule that led to an allogeneic barrier. This approach provided a new idea for cell transplantation in general.[38] However, the foreign body reaction caused by the silicone rubber tube is weak, the ability to form a fibrous capsule and blood vessels is limited, and it is more traumatic than injectable materials. To date, the majority of research on cell transplantation using fibrous capsules as barriers has been performed in islet transplantation approaches with obvious advantages. Whether this strategy can be applied in bone regeneration approaches is currently not clear and deserves further research.

To address the above-mentioned problems, immunocompe-tent mice were used to mimic immunocompetent humans as research subjects, aiming at providing an adaptive micro-environment for in vivo transplantation of hBMSCs and at contributing to bone differentiation with functionalized biomaterials as well as vascularized capsular tissues, so as to improve the compatibility and integration of exogenous stem cells into host tissue cells. For this, first, the functionalized hydrogel is injected into the subcutaneous tissue of the animal to form a fibrous cavity, and afterward, a part of the functionalized hydrogel is withdrawn. The remainder serves as a scaffold for cell adhesion to form a bioactive cell transplantation bed containing functionalized hydrogel and vascularized tissues; as soon as this is achieved, a sufficient number of cells in suspension is injected into the subcutaneous transplantation beds to allow for adherence, proliferation, and differentiation within the ectopic site. Finally, the vascularized bonelike tissues are surgically removed from the cell trans-plantation site and are used for regeneration and repair of large bone tissue defects.

2. MATERIALS AND METHODS

2.1. Purification of Sodium Alginate. Sodium alginate (SA) with high mannuronic acid content (G/M ≈ 0.64) and calcium sulfate powder were purchased from Sigma-Aldrich (St. Louis). To reduce the influence of impurities in the material on the experimental results and to ensure the maximum accuracy of the experiments, a gradient filtration method was used to purify sodium alginate under aseptic conditions. Sodium alginate was dissolved in deionized water and filtered through 0.8, 0.45, and 0.22 μm microporous membranes, respectively. The purified sodium alginate was obtained by freeze-drying the filtered sodium alginate solution.

2.2. Preparation of Alginate Hydrogels. As reported previously,[39] the RGD (RA) and QK-functionalized alginate (QA) to promote cell adhesion and angiogenesis was prepared by the carbodiimide chemistry method. Briefly, EDC and sulfo-NHS were reacted with alginate solution in MES buffer to form a stable intermediate, RGD/QK was added to the solution, and the resulting mixture was allowed to react at room temperature overnight. The final RGD/QK concentration was 1 mM. Following the peptide modification, the alginate was dialyzed (3.5 kDa), sterile-filtered (0.22 μm), and freeze-dried.

To prepare RA, QA, and RAQA (RA/QA = 1:1), calcium sulfate slurry (1.22 M in deionized water) was mixed with 2% (wt) modified alginate solution using Luer lock syringes and cross-linked between two glass plates that were separated by a 2 mm spacer. After cross-linking for 15 min, hydrogel matrix disks that were 2 mm in thickness and 14 mm in diameter were punched out with a metal punch. 2-(N-morpholino) ethanesulfonic acid (MES), N-hydroxy-sulfosuccinimide (sulfo-NHS), and 1-(3-dimethylaminopropyl)-3-ethylcarbodiimide (EDC) were obtained from Aladdin Reagent Co. Ltd. (Shanghai, China). The RGD peptide (GGGGRGDASSP sequence) and QK peptide (KLTWQELYQLKYKGI sequence) were synthesized by a batch-wise fmoc-polyamide method to achieve a greater than 98% purity.

2.3. Cell Culture. hBMSCs were purchased from ScienCell Research Laboratories (Carlsbad, CA) and maintained in high-glucose Dulbecco's modified Eagle's medium (DMEM; Hyclone) supplemented with 10% fetal bovine serum (Gibco, NY) and 1% penicillin/streptomycin (Gibco). The cells of passages 4−5 were used for the experiments. After 3 days of cell culture, the proliferation medium was exchanged against osteogenesis induction medium (low-glucose DMEM supplemented with 10 mM b-glycerol phosphate, 50 mg/mL ascorbic acid, and 0.1 mM dexamethasone; all from Sigma-Aldrich).

For alginate-based 3D culture studies, hBMSCs in the dish were trypsinized with 0.05% trypsin/EDTA (Gibco) and resuspended in serum-free medium. Subsequently, a Luer lock syringe was used to thoroughly mix the cell suspension with different alginate solutions. Then, the cell-alginate solution (3×10^6 cells per mL in alginate) was quickly mixed with calcium sulfate and injected into the mold. The cell-loaded hydrogel was transferred to a low-viscosity 24-well plate (Costar) and immersed in 1.5 mL of proliferation medium.

2.4. Proliferation of hBMSCs. The CCK-8 assay was used to evaluate the viability of the hBMSCs. Briefly, after incubation for 1, 3,
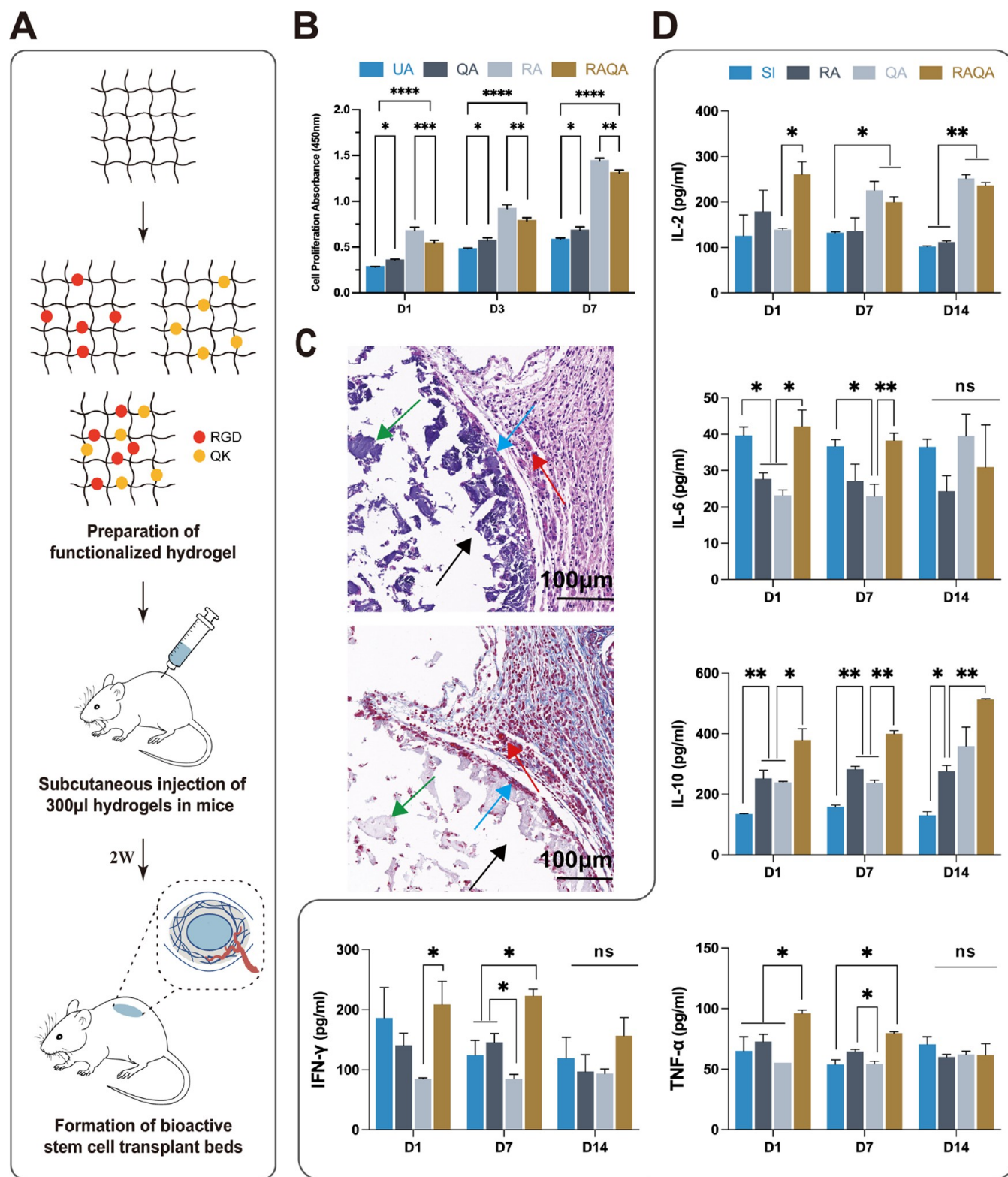
Figure 1. Construction and evaluation of bioactive stem cell transplantation beds in mice. (A) Schematic diagram of material preparation and capsule construction. Red dots represent RGD peptides, and yellow dots represent QK peptides. (B) Proliferation of hBMSCs in different matrices for 1, 3, and 7 days (*$P < 0.05$, **$P < 0.01$, ***$P < 0.001$ and ****$P < 0.0001$, $n = 3$). (C) Histological evaluation of the cell transplantation beds. The upper figure shows H&E staining, and the lower figure shows Masson staining. Red arrows represent blood vessels, green arrows represent materials, blue arrows represent fibrous tissues surrounding the materials and black arrows represent cavities. The scale bar represents 100 μm. (D) Detection of inflammatory factors surrounding the functionalized alginate hydrogel (*$P < 0.05$, **$P < 0.01$, $n = 3$). UA represents unmodified alginate hydrogel, SI represents silicone rubber tube, RA represents RGD-modified alginate hydrogel, QA represents QK-modified alginate hydrogel, and RAQA represents RGD and QK co-modified alginate hydrogel.

and 7 days, 10% CCK-8 reagent was added to each well and allowed to react for 4 h. The absorbance value of the supernatant optical density (OD) was measured using a microplate reader (SpectraMax M5) at 450 nm.

2.5. Construction and Evaluation of Bioactive Stem Cell Transplantation Beds in Mice. BALB/c mice with normal immune function, male, 6−8 weeks old, purchased from Beijing Weitong Lihua experimental animal Co., Ltd., were used as experimental animals. All animal protocols used in the present study were reviewed and approved by the Animal Care and Use Committee of Peking University. The mice were randomly divided into four groups and implanted with silicone rubber tubes (SI), RA, QA, and RAQA, respectively. For general anesthesia, 1% sodium pentobarbital solution was injected intraperitoneally into the mice prior to implantation with a calculated dose of 40 mg/kg of mouse body weight. After the mice were completely anesthetized, a small subcutaneous incision in the abdomen was made and a 2 cm long silicone rubber tube implant was inserted, after which the incision was closed. The procedure for the other hydrogel groups was the same, except that the mice were injected 300 μL of hydrogel using a 1 mL syringe instead of implanting a silicon rubber tube. Two weeks after implantation, the mice were anesthetized, and for the hydrogel groups, a syringe was inserted into the implant material and some hydrogel was extracted by first washing with normal saline and afterward, a part of the cell transplantation bed was prepared; for the SI group, the silicone rubber tube was removed. The mice were placed on a constant temperature table, and their status was closely surveyed until they awoke and left. All implants, surgical equipment, and surgical environment were strictly sterile and clean.

On postoperative days 1, 7, and 14, the mice were executed by cervical dislocation, the tissue blocks around the implants were cut out and placed in centrifuge tubes, added up with an appropriate amount of 0.9% saline, and homogenized. The supernatant was recovered after centrifugation at 3000 rpm for 10 min. The inflammatory cytokines (IL-2, IL-6, IL-10, TNF-α, IFN-γ) contained in the supernatant were detected by an ELISA kit.

Tissue samples from mice 2 weeks after implantation of the material were fixed in 10% neutral formalin for 48 h. The samples were processed for paraffin sectioning, and the section (5 mm) was stained with hematoxylin and eosin (H&E) as well as Masson's trichrome staining method according to the manufacturer's protocol.

2.6. Formation and Evaluation of the Bonelike Tissues in Bioactive Stem Cell Transplantation Beds. After the bioactive stem cell transplantation beds were built, SI, RA, QA, and RAQA were stratified into three subgroups, namely, into the non-cell-transplanted (NO), the hBMSCs cultured in proliferation medium (CM), and hBMSCs cultured under osteogenic induction conditions (OM) transplantation group. Each transplantation site extended from the incision or needle hole to the stem cell transplantation beds, and 100 μL of cell suspension (3×10^7 cells per mL) was injected through a 1 mL syringe needle. We used a tacrolimus-based immunosuppression method (0.5 mg/kg/day) to suppress an immune reaction.

The mice were euthanized 4 weeks post-surgery, the tissue samples were excised, and fixed overnight in 10% neutral formalin (Solarbio, China). Total bone volume was visualized and quantified using a micro-computed tomography method (Micro CT). The samples were processed for paraffin sectioning and stained with H&E, Masson's trichrome staining, Safranin O−Fast Green staining, Alcian Blue staining, Sirius Red staining, and immunohistochemistry (IHC) staining following the respective manufacturer's protocols. The primary antibodies for IHC staining included antibodies against COL1A1 (ab90395), OPN (ab69498), RUNX2 (ab192256), vWF (ab9378), and COL2A1 (ab34712).

2.7. Statistical Analysis. The data are presented as mean ± standard deviation (SD). Using Origin 2019 software, one-way analysis of variance (ANOVA) followed by Tukey's test was performed to assess significant differences among groups. P-Values <0.05 (*) and <0.01 (**) indicated a statistically significant difference or a highly statistically significant difference, respectively.

3. RESULTS

3.1. Biocompatibility Evaluation of Functionalized Alginate Hydrogels In Vitro. We used a CCK-8 assay to detect hBMSCs proliferation after an incubation period of 1, 3, and 7 days as shown in Figure 1B. In the control group, the cells were cultured in unmodified alginate hydrogel (UA). The results showed that the OD values of all samples increased with time, indicating that the alginate hydrogel had no adverse effect on the proliferation of hBMSCs, whether modified or not. Peptides can provide adhesion sites for the cells in the materials; therefore, the cells in RA and RAQA were fully extended and showed good proliferative activity. In the RAQA group, we did not observe a significant decrease of proliferative activity after halving the RGD content and introducing the QK peptide, suggesting that the introduction of QK peptide had no obvious effect on cell proliferation. In conclusion, the functionalized sodium alginate hydrogel displayed good cytocompatibility and was evaluated as being appropriate for subsequent animal experiments.

3.2. Histological Evaluation and Inflammatory Factor Detection in Bioactive Stem Cell Transplantation Beds. *3.2.1. Histological Analysis.* To further investigate whether the implanted functionalized sodium alginate hydrogels produced bioactive stem cell transplantation beds, we performed an H&E and a Masson staining of paraffin sections of subcutaneous composite cystic tissues 2 weeks after material transplantation. Figure 1A shows a schematic representation of the material transplantation. As shown in Figure 1C, RAQA caused a moderate foreign body reaction in the host, leading to the formation of a fibrous layer encasing the hydrogel with many tiny blood vessels and erythrocytes visible in the lumen. Fragments of dark-blue-stained sodium alginate hydrogel were visible inside the material, which was due to the gradual degradation of the material in vivo; in the Masson staining, fuchsia-stained collagen fibers surrounding the hydrogel could be seen. Thus, 2 weeks after implantation of the hydrogel, a cell transplantation bed with blood vessels around the material was formed.

3.2.2. ELISA Analysis. IL-2 is used to treat autoimmune and inflammatory diseases and to promote immune tolerance. IL-10 is an anti-inflammatory cytokine that generally appears later in the inflammatory response. IL-6 is a pro-inflammatory cytokine that increases neutrophil production, stimulates lymphocyte proliferation and maturation, and promotes the expression of further pro-inflammatory cytokines. IFN-γ can upregulate pro-inflammatory cytokine expression and inhibit the secretion of anti-inflammatory cytokines. TNF-α is a common pro-inflammatory cytokine that activates and induces the release of other inflammatory mediators. As can be seen in Figure 1D, the QA group showed a gradual increase of IL-2 over time, while the other three groups showed a slight decrease or a more or less stable course over time. The RAQA group was less susceptible to immune rejection in the initial stage as indicated by the highest values for this group on day 1. The QA group displayed the highest values of IL-6 with a gradual increase over time, while RA and RAQA groups showed a slightly decreasing or essentially flat trend over time. Moreover, the RAQA group values were higher on days 1 and 7. For IL-2 and IL-6, the QA groups showed a gradual increase over time, while the RAQA group showed a slightly decreasing or essentially flat trend over time. For IL-10, there was a progressive increase in IL-10 secretion over time in the QA
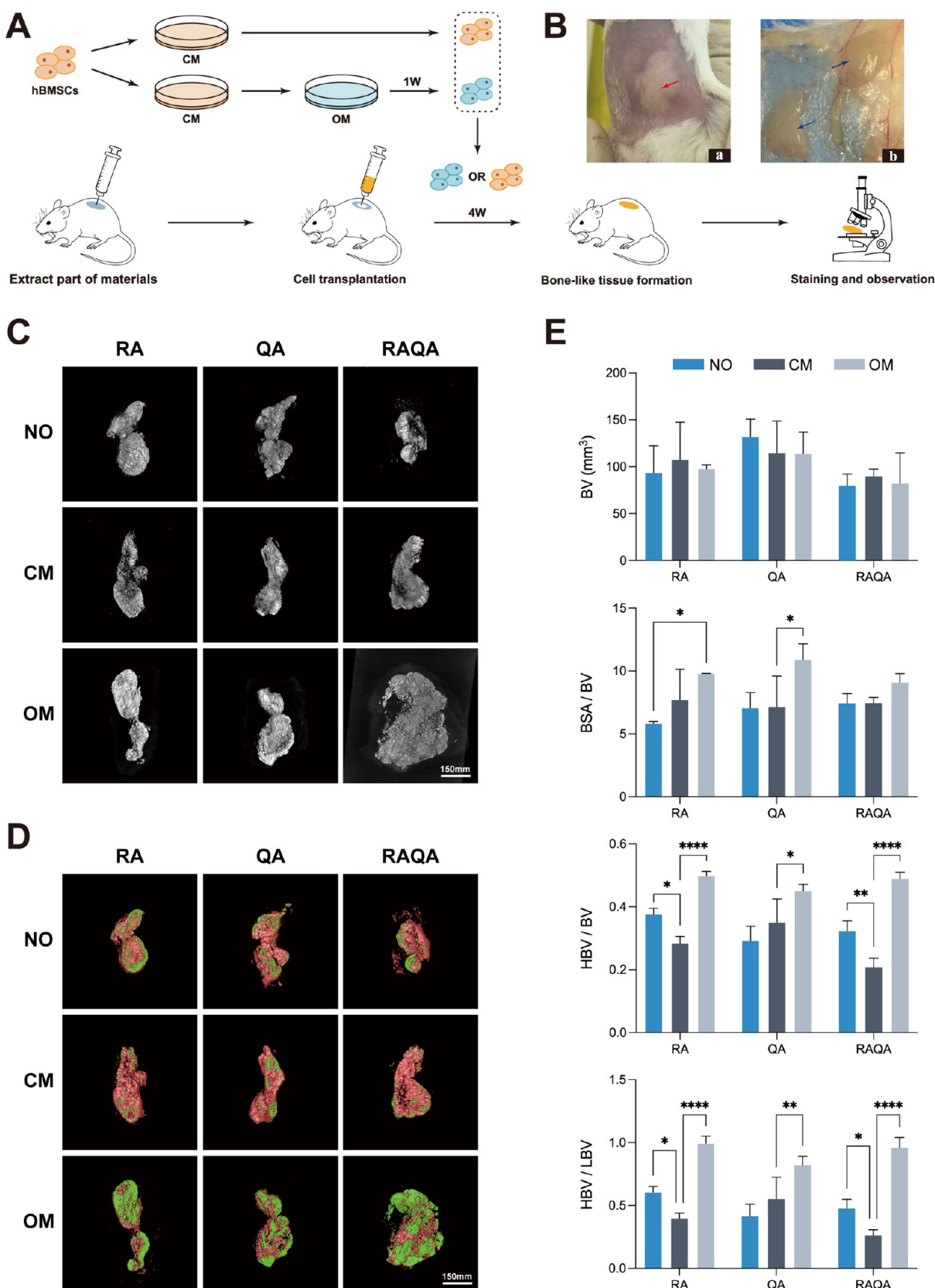
Figure 2. Micro CT analysis of bonelike tissues derived from implanted hBMSCs. (A) Schematic diagram of implanting cells into the bioactive transplantation beds. (B) Digital picture of the bioactive cell transplantation beds (a) and 4 weeks after hBMSCs implantation (b); the red arrow represents the bioactive transplantation beds, and the blue arrow represents bonelike tissues. (C, D) Screenshots of three-dimensional reconstructions using Micro CT analysis. Green represents high density (>2200 mg HA/cm^3); red represents low density (1200−2200 mg HA/cm^3). (E) Quantitative Micro CT analysis. (*P < 0.05, **P < 0.01, and ***P < 0.001, n = 3). NO represents non-cell transplanted, CM represents the hBMSCs cultured in proliferation medium, and OM represents the hBMSCs cultured under osteogenic induction conditions.

and RAQA groups, while the SI and RA group courses were essentially flat over time, which is consistent with a later appearance in the inflammatory response. The secretion of TNF-α was significantly higher in the RAQA group on day 1 but gradually leveled with the other groups over time. The secretion of IFN-γ was lowest in the QA group and highest in the RAQA group. By analyzing the ELISA data, we found that SI induced a similar foreign body response to RA and the RAQA group caused more pro-inflammatory factors (TNF-α and IFN-γ) secreted than the other groups and the intensity of the foreign body response was more pronounced, thus also facilitating the formation of a fibrous composite cystic cavity around the material.

3.3. Evaluation of the Bone Regeneration Capacity of hBMSCs in Bioactive Stem Cell Transplantation Beds.

3.3.1. Micro CT Analysis. Four weeks after cell implantation, we analyzed the samples by Micro CT. A high image density represents bone tissue, and the brighter the image, the higher the hardness of the bone tissue. We found that bone regeneration was visible in the bioactive stem cell transplantation beds, whether the cells were treated with osteogenic induction (Figure 2C) or not. The images taken from the OM group revealed a high density at the edges of the construct, which to some extent shows that this group has a stronger ability to form high-density bone at the edges. This is also true for natural bone tissue, displaying a higher density in the bone cortex than in cancellous bone regions. Figure 2D represents cross-sectional views of samples of each group in which the green and red areas indicate high-density and low-density bone regions, respectively. We detected no significant difference in the red and green stained areas between the RA, QA, and RAQA groups, respectively. In contrast, significant differences could be shown in the comparison of the NO, CM, and OM groups, respectively. The area of high-density bone in the OM group was significantly larger than that in the other two groups. However, there were no significant differences between the high- and low-density bone areas of the NO and CM groups, which could be characterized as having a larger low-density bone area. Figure 2E shows the quantitative data of the Micro CT 3D scanning analysis. Here, a common denominator was the fact that when the in vitro culture conditions of the transplanted cells were the same, the RA, QA, and RAQA groups showed a significant bone regeneration ability with no differences between the three hydrogel groups. The quantitative analysis of bone volume (BV) showed that the amount of bone formed by the bioactive stem cell transplantation beds was higher and independent of the prior in vitro culture conditions of the cells. The quantitative analysis of the bone surface area specific bone volume (BSA/BV) showed that the degree of bone formation in the RAQA group was independent of the prior in vitro culture conditions of the transplanted cells. However, there was a significant difference between the RA and QA groups under OM and NO conditions that displayed a larger relative surface area. The quantitative analysis of the ratio of high-density bone volume to bone volume (HBV/BV) and the ratio of high-density to low-density bone volume (HBV/LBV) showed that the OM group had the highest bone quality in the different hydrogel groups. Taken together, we could show that 4 weeks after implantation of the cells into the bioactive transplantation beds, new bone formation occurred in the RA, QA, and RAQA groups and that the regeneration ability of the transplanted cells cultivated in

vitro under bone induction conditions was better than that of cells that were cultivated under noninduction.

3.3.2. Histological Analysis. Figure 3A,B shows the results of an H&E and MASSON staining 4 weeks after cell
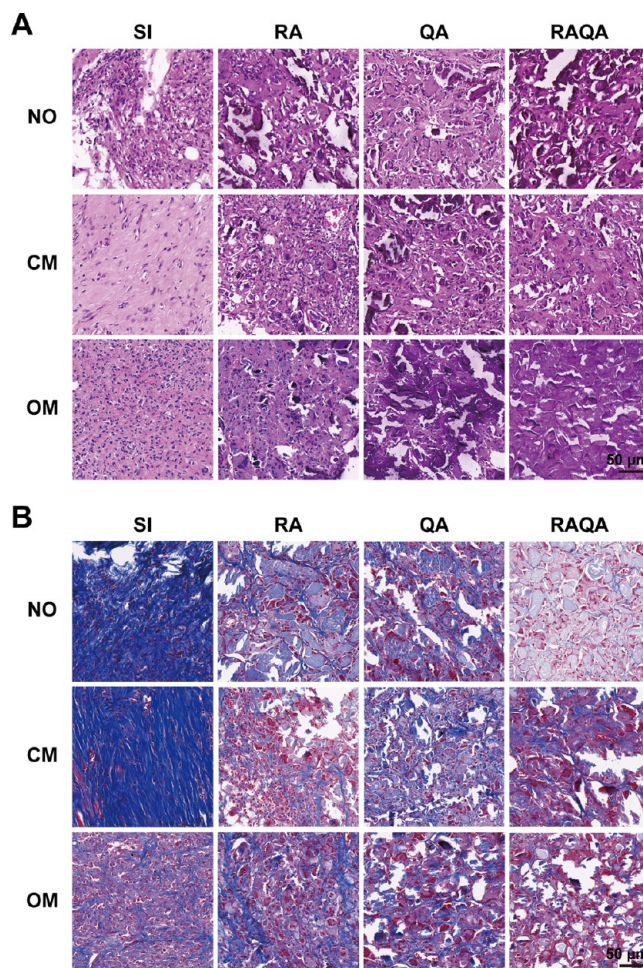
Figure 3. Histological evaluation of bonelike tissues 4 weeks after cell implantation. (A) H&E staining and (B) Masson staining. The scale bar represents 50 μm.

transplantation. We found that the bone regeneration ability of each hydrogel group was better than that of the SI group and that the ability of bone regeneration was better than that of the other two groups under OM conditions. This is due to the differentiation of cells into osteoblasts after osteogenic induction and their improved matrix secretion capacity. For the OM−RAQA group, the one with the best osteogenic effect, Alizarin Red S staining (Figure 4A), Safranin O−Fast Green staining (Figure 4B), Alcian Blue staining (Figure 4C), and Sirius Red staining (Figure 4D) were carried out. As a result, we found that the bonelike tissues formed displayed COL2A1 and glycosaminoglycan deposition in the capsule wall and the capsule itself. This shows that osteoid tissue has the potential for endochondral osteogenesis. Sirius red staining showed that there were type I and type III collagen fibers in the bonelike tissue close to the capsule wall, indicating that the bonelike tissue may be in the stage of bone formation with bone matrix deposition and vascular migration.

3.3.3. Immunohistochemical Analysis. RUNX2, positively correlating with intramembranous and endochondral ossifica-
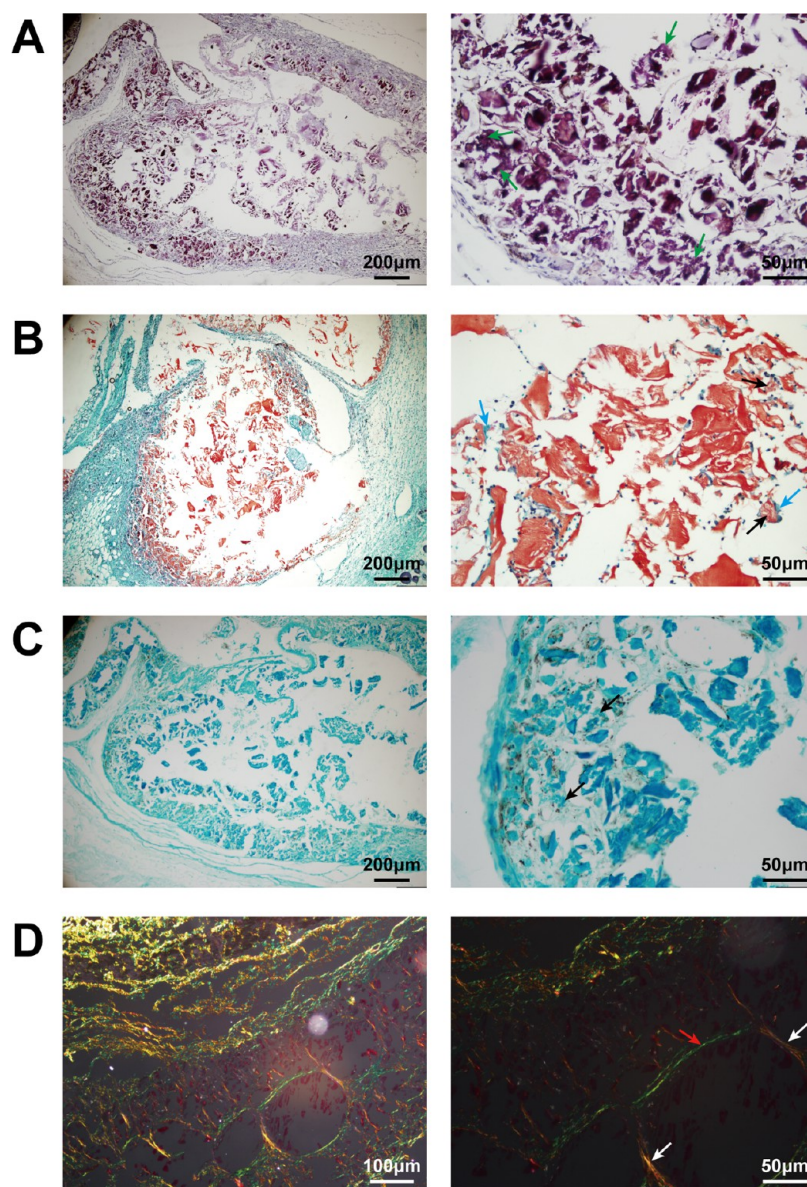
Figure 4. Histological evaluation of vascularized bonelike tissues components in OM−RAQA group. (A) Alizarin Red S staining; (B) Safranin O−Fast Green staining; (C) Alcian Blue staining; (D) Sirius Red staining. The green arrow represents calcium nodule formation, the blue arrow represents COL2A1, the black arrow represents glycosaminoglycan, the white arrow represents COL1A1, and the red arrow represents type III collagen.

tion, can upregulate the expression of several osteogenesis-related genes, while COL1A1 and OPN play a rather important role in bone matrix formation and mineralization. Figures 5A,B, and 6A show the immunohistochemical stainings of type I collagen fibers (COL1A1), OPN, and RUNX2, respectively. The osteogenic ability of each hydrogel group was better than that of the other two conditions, especially in the RAQA group, where we could see a higher expression of RUNX2 and more production of COL1A1 and OPN. Figure 6B shows the results of immunohistochemical staining of vWF, which revealed that the angiogenic ability of each hydrogel group was better than that of the SI group. This might be due to the fact that QK peptides can effectively recruit vascular endothelial cells to migrate into the capsule. Compared to the SI group, the angiogenic ability of each hydrogel group under different cell transplantation conditions showed that the angiogenic ability of cells under OM conditions was better

than that of the other two groups, especially the RAQA group showed angiogenesis in the compound capsule. Moreover, the results showed that the composite capsule of RAQA can grow into bonelike tissue from blood vessels by transplanting hBMSCs under OM conditions, avoiding the problem of bone necrosis caused by a lack of blood supply in the osteogenic center during osteogenesis. For the OM group, we stained COL2A1 for each material group. It can be seen from Figure 6C that the RAQA group showed a higher COL2A1 expression, which is consistent with the results of the histological staining and which indicates that the vascularized bonelike tissues have the ability to form bone tissue through endochondral osteogenesis.

4. DISCUSSION

Stem cell-based therapies have great potential in the field of bone tissue regeneration, but the survival and functioning of
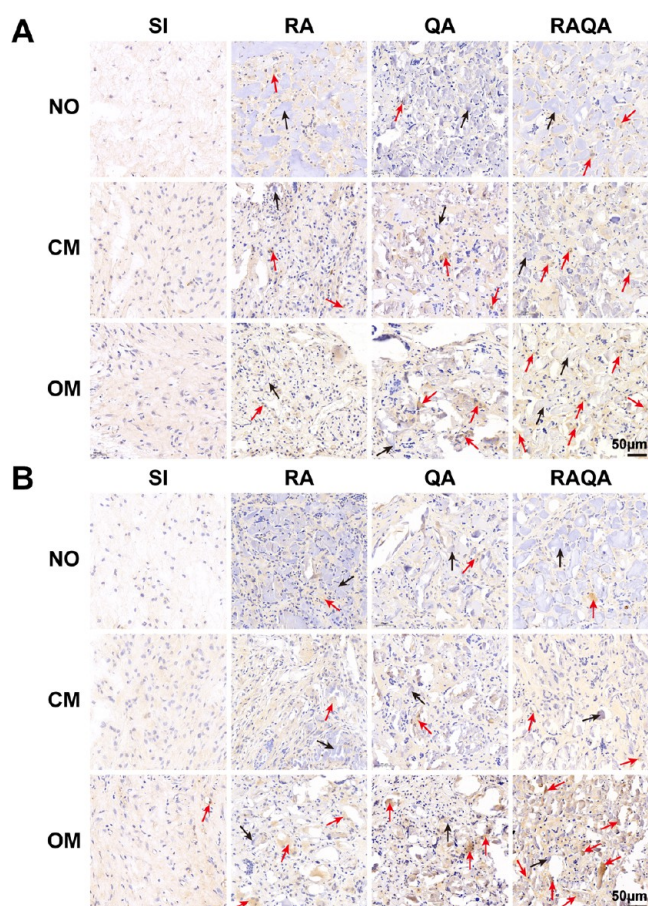
Figure 5. Immunohistochemical analysis of components associated with intramembranous ossification in vascularized bonelike tissues. (A) IHC staining against COL1A1 and (B) IHC staining against OPN. Red arrows represent brown-stained positive tissues, and black arrows point to materials. The scale bar represents 50 μm.

Figure 6. Immunohistochemical analysis of components associated with endochondral ossification in vascularized bonelike tissues. (A) IHC staining against RUNX2; (B) IHC staining against vWF; and (C) IHC staining against COL2A1 in the OM group. Red arrows represent brown-stained positive tissues, and black arrows point to materials. The scale bar represents 50 μm.

transplanted cells within the host tissue is one of the greatest challenges with regard to clinical translation. When stem cells are injected into host tissue, they will spread from the target area after transplantation and implantation in vivo,[40] and due to the lack of an adaptive microenvironment, the cells lack material exchange,[41] hypoxia,[42] and finally lead to cell loss of nest and apoptosis.[43] In this study, we provided a more efficient, simple, and minimally invasive method for cell transplantation using RGD and QK co-modified sodium alginate hydrogels injected subcutaneously into mice to form bioactive cell transplantation beds. The transplantation beds provide resident space, RGD peptides provide adhesion sites, and QK peptides provide a vascularized microenvironment for cells to satisfy the need for survival and function. The effect of implanted biomaterials usually depends on their interaction with the host immune system, including blood–material interaction, temporary matrix formation, persistent immune response, chronic immune response, granulation tissue, and fibrous capsule formation.[44−47] During this process, inflammatory monocytes and resident tissue macrophages play an indispensable role in tissue repair, regeneration, and fibrosis.[48,49] Macrophages have been categorized conventionally into pro-inflammatory M1 and tissue-repairing M2 phenotypes. "Classically activated" macrophages are irreplaceable, protecting the individual and fighting intracellular bacteria or viruses by producing nitric oxide, reactive oxygen

species (ROS), pro-inflammatory mediators, and chemokines, such as interleukin-1 (IL-1), TNF-a, and IL-10.[50] After the acute phase of tissue injury, a switch in the predominant macrophage phenotype to the "nonclassical" or wound-healing phenotype occurs through signaling by IL-6 and TNF-a signaling that is both immunomodulatory and profibrotic.[51] Furthermore, foreign body giant cells also activate M2-type macrophages by secreting IL-10 which promotes fibrosis.[52] In this study, we used the host's own foreign body reaction to prepare the bioactive cell transplantation beds by the functionalized alginate hydrogel and found that IL-2 and IL-6 tended to decrease slightly or remained essentially low over time; it was highest in the RAQA group on day 1, suggesting that this group is less susceptible to immune rejection during the initial phase. The RAQA group secreted more pro-inflammatory factors (TNF-α and IFN-γ) than the other groups, which also facilitated the formation of fibrous composite cysts around the material.

Blood vessels play a central role in the process of bone regeneration. In the early stages of bone regeneration, the blood vessels adjacent to BMSCs provide access to oxygen, various circulating electrolytes, proteins, gases, lipids, pluripotent cells, and minerals, including calcium and phosphate ions essential for osteogenesis.[53] Maes showed that some osteoblast precursors exhibit a perivascular localization, confirming a strong relationship between angiogenesis and osteogenesis.[54] Interestingly, Ben Shoham demonstrated that during embryonic development, endothelial cells are instead covered by the osteoblast-secreted collagen type I and can undergo gradual mineralization, thus serving as a mineralization template.[55] This study suggests that bone vasculature can serve as a guiding template for mineralized bone deposition. Our results showed that the bioactive cell transplantation beds were highly vascularized using RAQA, and after transplantation of hBMSCs, Micro CT analysis revealed that HBV of the vascularized bonelike tissues formed was higher than that of RA and QA groups, demonstrating a higher degree of bone mineralization. Immunohistochemical analysis revealed a significant upregulation of RUNX2 expression together with a high COL1A1 and OPN expression. This result is consistent with previous studies and suggests that it allows easier contact with the surrounding tissue of the bone defect through the internal blood vessels.

There are two different ways of bone regeneration.[56] One is intramembrane osteogenesis, in which mesenchymal stem cells aggregate into spheres and differentiate directly into osteoblasts. The other is endochondral osteogenesis. To achieve this, mesenchymal stem cells first aggregate and differentiate into chondrocytes. Upon chondrocyte maturation and hypertrophy, they are finally transformed into osteoblasts. The process of bone healing in its early stage is characterized by a hematoma microenvironment with hypoxia and low pH.[57] Within this environment, mesenchymal stem cells are more likely to differentiate into chondrocytes and mainly participate in osteogenic repair through endochondral osteogenesis. In the middle stage of the bone defect repair, with the beginning of revascularization, intramembrane osteogenesis gradually becomes the main repair pathway. This study showed that hBMSCs not only have the ability of intramembrane ossification but also have the ability of endochondral ossification in the bioactive stem cell transplantation beds. We speculate that when cells are implanted into the capsule cavity, some cells adhere to the capsule wall. Because the capsule wall provides abundant nutrients and oxygen for hBMSCs via the blood vessels contained therein, it is more conducive to the differentiation of hBMSCs into osteoblasts through intramembrane osteogenesis. Some cells adhere to the materials in the capsule and do not contact the capsule wall. Due to the lack of nutrients and oxygen in the capsule, hBMSCs tend to form bone tissue through endochondral ossification. The difference in the extracellular microenvironment then drives the hBMSCs into multidirectional differentiation.

5. CONCLUSIONS

In this study, we provided a novel cell transplantation strategy for bone regeneration using functionalized sodium alginate hydrogels injected subcutaneously into immunocompetent mice to form bioactive cell transplantation beds and obtain vascularized bonelike tissues with hBMSCs injected in beds. This approach not only allows for efficient, minimally invasive, and convenient construction of subcutaneous cell transplantation beds but also reduces cell death using the residual hydrogel to provide adhesion sites for the transplanted cells. The transplanted cells can gradually adapt to the microenvironment in the transplantation beds to avoid the influence of immune rejection in the early stage of transplantation. The blood vessels in the capsule wall provide nutrition for the cells and ensure their proliferation and metabolism. The functionalized sodium alginate retained in the capsule can be used as a biological scaffold to provide a microenvironment for cell adhesion, proliferation, and directed differentiation. In vivo studies demonstrated that RGD and QK peptides co-modified with sodium alginate hydrogel, including differentiation-induced hBMSCs, showed a higher expression of not only hemophilia angiogenic factor but also osteogenesis- and chondrogenesis-related proteins. These results suggest that the bioactive cell transplantation beds can provide an adaptive microenvironment in vivo to facilitate cell viability and osteogenic differentiation for exogenous cell transplantation. The vascularized bonelike tissues formed in the bioactive cell transplantation beds have the potential for intramembrane and endochondral ossification, which can be used for further in situ transplantation into large bone defects. Therefore, this cell transplantation strategy is promising for use in bone tissue defects of larger animals, especially for providing a graft embryo for large bone defect repairs.

■ AUTHOR INFORMATION

Corresponding Author

Shicheng Wei − Central Laboratory, and Department of Oral and Maxillofacial Surgery, School and Hospital of Stomatology, Peking University, Beijing 100081, P. R. China; Laboratory of Biomaterials and Regenerative Medicine, Academy for Advanced Interdisciplinary Studies, Peking University, Beijing 100871, P. R. China; orcid.org/0000-0001-6024-9615; Email: sc-wei@pku.edu.cn

Authors

He Zhang − Central Laboratory, and Department of Oral and Maxillofacial Surgery, School and Hospital of Stomatology, Peking University, Beijing 100081, P. R. China

Xiaoming Fu − Central Laboratory, and Department of Oral and Maxillofacial Surgery, School and Hospital of Stomatology, Peking University, Beijing 100081, P. R. China

Siqi Zhang − Laboratory of Biomaterials and Regenerative Medicine, Academy for Advanced Interdisciplinary Studies, Peking University, Beijing 100871, P. R. China

Qian Li − Laboratory of Biomaterials and Regenerative Medicine, Academy for Advanced Interdisciplinary Studies, Peking University, Beijing 100871, P. R. China

Yang Chen − Laboratory of Biomaterials and Regenerative Medicine, Academy for Advanced Interdisciplinary Studies, Peking University, Beijing 100871, P. R. China

Hao Liu − Central Laboratory, and Department of Oral and Maxillofacial Surgery, School and Hospital of Stomatology, Peking University, Beijing 100081, P. R. China

Wen Zhou − Central Laboratory, and Department of Oral and Maxillofacial Surgery, School and Hospital of Stomatology, Peking University, Beijing 100081, P. R. China

Complete contact information is available at:
https://pubs.acs.org/10.1021/acsbiomaterials.1c01512

■ REFERENCES

(1) Calori, G.; Mazza, E.; Colombo, M.; Ripamonti, C. The use of bone-graft substitutes in large bone defects: any specific needs? *Injury* **2011**, *42*, S56−S63.

(2) Lasanianos, N. G.; Kanakaris, N. K.; Giannoudis, P. V. Current management of long bone large segmental defects. *Orthop. Traumatol.* **2010**, *24*, 149−163.

(3) Walmsley, G. G.; Ransom, R. C.; Zielins, E. R.; Leavitt, T.; Flacco, J. S.; Hu, M. S.; Lee, A. S.; Longaker, M. T.; Wan, D. C. Stem Cells in Bone Regeneration. *Stem Cell Rev. Rep.* **2016**, *12*, 524−529.

(4) Bishop, J. A.; Palanca, A. A.; Bellino, M. J.; Lowenberg, D. W. Assessment of compromised fracture healing. *J. Am. Acad. Orthop. Surg.* **2012**, *20*, 273−282.

(5) Lin, C. Y.; Wang, Y. H.; Li, K. C.; Sung, L. Y.; Yeh, C. L.; Lin, K. J.; Yen, T. C.; Chang, Y. H.; Hu, Y. C. Healing of massive segmental femoral bone defects in minipigs by allogenic ASCs engineered with FLPo/Frt-based baculovirus vectors. *Biomaterials* **2015**, *50*, 98−106.

(6) Fan, H.; Zeng, X.; Wang, X.; Zhu, R.; Pei, G. Efficacy of prevascularization for segmental bone defect repair using β-tricalcium phosphate scaffold in rhesus monkey. *Biomaterials* **2014**, *35*, 7407−7415.

(7) Ashman, O.; Phillips, A. Treatment of non-unions with bone defects: which option and why? *Injury* **2013**, *44*, S43−S45.

(8) Ball, A. N.; Donahue, S. W.; Wojda, S. J.; McIlwraith, C. W.; Kawcak, C. E.; Ehrhart, N.; Goodrich, L. R. The challenges of promoting osteogenesis in segmental bone defects and osteoporosis. *J. Orthop. Res.* **2018**, *36*, 1559−1572.

(9) Fitoussi, F.; Masquelet, A. C.; Rigal, S.; Poichotte, A.; Bauer, T.; Fabre, A. French Society of, O.; Traumatologic, S., Inter-tibiofibular graft for traumatic segmental bone defect of the tibia. *Orthop. Traumatol. Surg. Res.* **2012**, *98*, 214−219.

(10) Moura, L. B.; Carvalho, P. H.; Xavier, C. B.; Post, L. K.; Torriani, M. A.; Santagata, M.; Chagas Junior, O. L. Autogenous non-vascularized bone graft in segmental mandibular reconstruction: a systematic review. *Int. J. Oral Maxillofac. Surg.* **2016**, *45*, 1388−1394.

(11) Moore, W. R.; Graves, S. E.; Bain, G. I. Synthetic bone graft substitutes. *ANZ J. Surg.* **2001**, *71*, 354−361.

(12) Hutmacher, D. W. Scaffolds in tissue engineering bone and cartilage. *Biomaterials* **2000**, *21*, 2529−2543.

(13) Oryan, A.; Alidadi, S.; Bigham-Sadegh, A.; Meimandi-Parizi, A. Chitosan/gelatin/platelet gel enriched by a combination of hydroxyapatite and beta-tricalcium phosphate in healing of a radial bone defect model in rat. *Int. J. Biol. Macromol.* **2017**, *101*, 630−637.

(14) Kim, S.; Bedigrew, K.; Guda, T.; Maloney, W. J.; Park, S.; Wenke, J. C.; Yang, Y. P. Novel osteoinductive photo-cross-linkable chitosan-lactide-fibrinogen hydrogels enhance bone regeneration in critical size segmental bone defects. *Acta Biomater.* **2014**, *10*, 5021−5033.

(15) Zheng, C.; Chen, J.; Liu, S.; Jin, Y. Stem cell-based bone and dental regeneration: a view of microenvironmental modulation. *Int. J. Oral Sci.* **2019**, *11*, No. 23.

(16) Ho-Shui-Ling, A.; Bolander, J.; Rustom, L. E.; Johnson, A. W.; Luyten, F. P.; Picart, C. Bone regeneration strategies: Engineered scaffolds, bioactive molecules and stem cells current stage and future perspectives. *Biomaterials* **2018**, *180*, 143−162.

(17) Lyons, F. G.; Al-Munajjed, A. A.; Kieran, S. M.; Toner, M. E.; Murphy, C. M.; Duffy, G. P.; O'Brien, F. J. The healing of bony defects by cell-free collagen-based scaffolds compared to stem cell-seeded tissue engineered constructs. *Biomaterials* **2010**, *31*, 9232−9243.

(18) Gupta, K.; Gupta, P.; Wild, R.; Ramakrishnan, S.; Hebbel, R. P. Binding and displacement of vascular endothelial growth factor (VEGF) by thrombospondin: effect on human microvascular endothelial cell proliferation and angiogenesis. *Angiogenesis* **1999**, *3*, 147−158.

(19) Cai, L.; Dinh, C. B.; Heilshorn, S. C. One-pot Synthesis of Elastin-like Polypeptide Hydrogels with Grafted VEGF-Mimetic Peptides. *Biomater. Sci* **2014**, *2*, 757−765.

(20) Webber, M. J.; Tongers, J.; Newcomb, C. J.; Marquardt, K.-T.; Bauersachs, J.; Losordo, D. W.; Stupp, S. I. Supramolecular nanostructures that mimic VEGF as a strategy for ischemic tissue repair. *Proc. Natl. Acad. Sci. U.S.A.* **2011**, *108*, 13438−13443.

(21) Finetti, F.; Basile, A.; Capasso, D.; Di Gaetano, S.; Di Stasi, R.; Pascale, M.; Turco, C. M.; Ziche, M.; Morbidelli, L.; D'Andrea, L. D. Functional and pharmacological characterization of a VEGF mimetic peptide on reparative angiogenesis. *Biochem. Pharmacol.* **2012**, *84*, 303−311.

(22) Santulli, G.; Ciccarelli, M.; Palumbo, G.; Campanile, A.; Galasso, G.; Ziaco, B.; Altobelli, G. G.; Cimini, V.; Piscione, F.; D'Andrea, L. D.; Pedone, C.; Trimarco, B.; Iaccarino, G. In vivo properties of the proangiogenic peptide QK. *J. Transl. Med.* **2009**, *7*, No. 41.

(23) Yang, Y.; Yang, Q.; Zhou, F.; Zhao, Y.; Jia, X.; Yuan, X.; Fan, Y. Electrospun PELCL membranes loaded with QK peptide for enhancement of vascular endothelial cell growth. *J. Mater. Sci. Mater. Med.* **2016**, *27*, No. 106.

(24) Chan, T. R.; Stahl, P. J.; Yu, S. M. Matrix-Bound VEGF Mimetic Peptides: Design and Endothelial Cell Activation in Collagen Scaffolds. *Adv. Funct. Mater.* **2011**, *21*, 4252−4262.

(25) Leslie-Barbick, J. E.; Saik, J. E.; Gould, D. J.; Dickinson, M. E.; West, J. L. The promotion of microvasculature formation in poly(ethylene glycol) diacrylate hydrogels by an immobilized VEGF-mimetic peptide. *Biomaterials* **2011**, *32*, 5782−5789.

(26) Mendicino, M.; Bailey, A. M.; Wonnacott, K.; Puri, R. K.; Bauer, S. R. MSC-based product characterization for clinical trials: an FDA perspective. *Cell Stem Cell* **2014**, *14*, 141−145.

(27) Trounson, A.; McDonald, C. Stem cell therapies in clinical trials: progress and challenges. *Cell Stem Cell* **2015**, *17*, 11−22.

(28) Heathman, T. R.; Nienow, A. W.; McCall, M. J.; Coopman, K.; Kara, B.; Hewitt, C. J. The translation of cell-based therapies: clinical landscape and manufacturing challenges. *Regener. Med.* **2015**, *10*, 49−64.

(29) Harrell, C. R.; Markovic, B. S.; Fellabaum, C.; Arsenijevic, A.; Volarevic, V. Mesenchymal stem cell-based therapy of osteoarthritis: Current knowledge and future perspectives. *Biomed. Pharmacother.* **2019**, *109*, 2318−2326.

(30) Wang, Y.; Tian, M.; Wang, F.; Heng, B. C.; Zhou, J.; Cai, Z.; Liu, H. Understanding the immunological mechanisms of mesenchymal stem cells in allogeneic transplantation: from the aspect of

major histocompatibility complex class I. *Stem Cells Develop.* **2019**, *28*, 1141−1150.

(31) Jin, S. S.; He, D. Q.; Luo, D.; Wang, Y.; Yu, M.; Guan, B.; Fu, Y.; Li, Z. X.; Zhang, T.; Zhou, Y. H.; Wang, C. Y.; Liu, Y. A Biomimetic Hierarchical Nanointerface Orchestrates Macrophage Polarization and Mesenchymal Stem Cell Recruitment To Promote Endogenous Bone Regeneration. *ACS Nano* **2019**, *13*, 6581−6595.

(32) Maia, F. R.; Fonseca, K. B.; Rodrigues, G.; Granja, P. L.; Barrias, C. C. Matrix-driven formation of mesenchymal stem cell-extracellular matrix microtissues on soft alginate hydrogels. *Acta Biomater.* **2014**, *10*, 3197−3208.

(33) Ho, S. S.; Murphy, K. C.; Binder, B. Y.; Vissers, C. B.; Leach, J. K. Increased Survival and Function of Mesenchymal Stem Cell Spheroids Entrapped in Instructive Alginate Hydrogels. *Stem Cells Transl. Med.* **2016**, *5*, 773−781.

(34) Li, Y.; Luo, Z.; Xu, X.; Li, Y.; Zhang, S.; Zhou, P.; Sui, Y.; Wu, M.; Luo, E.; Wei, S. Aspirin enhances the osteogenic and anti-inflammatory effects of human mesenchymal stem cells on osteogenic BFP-1 peptide-decorated substrates. *J. Mater. Chem. B* **2017**, *5*, 7153−7163.

(35) Xu, X.; Wang, L.; Luo, Z.; Ni, Y.; Sun, H.; Gao, X.; Li, Y.; Zhang, S.; Li, Y.; Wei, S. Facile and Versatile Strategy for Construction of Anti-Inflammatory and Antibacterial Surfaces with Polydopamine-Mediated Liposomes Releasing Dexamethasone and Minocycline for Potential Implant Applications. *ACS Appl. Mater. Interfaces* **2017**, *9*, 43300−43314.

(36) Luo, Z.; Pan, J.; Sun, Y.; Zhang, S.; Yang, Y.; Liu, H.; Li, Y.; Xu, X.; Sui, Y.; Wei, S. Injectable 3D Porous Micro-Scaffolds with a Bio-Engine for Cell Transplantation and Tissue Regeneration. *Adv. Funct. Mater.* **2018**, *28*, No. 1804335.

(37) Luo, Z.; Zhang, S.; Pan, J.; Shi, R.; Liu, H.; Lyu, Y.; Han, X.; Li, Y.; Yang, Y.; Xu, Z.; Sui, Y.; Luo, E.; Zhang, Y.; Wei, S. Time-responsive osteogenic niche of stem cells: A sequentially triggered, dual-peptide loaded, alginate hybrid system for promoting cell activity and osteo-differentiation. *Biomaterials* **2018**, *163*, 25−42.

(38) Pepper, A. R.; Gala-Lopez, B.; Pawlick, R.; Merani, S.; Kin, T.; Shapiro, A. J. A prevascularized subcutaneous device-less site for islet and cellular transplantation. *Nat. Biotechnol.* **2015**, *33*, 518−523.

(39) Rowley, J. A.; Madlambayan, G.; Mooney, D. J. Alginate hydrogels as synthetic extracellular matrix materials. *Biomaterials* **1999**, *20*, 45−53.

(40) Williams, C. G.; Kim, T. K.; Taboas, A.; Malik, A.; Manson, P.; Elisseeff, J. In vitro chondrogenesis of bone marrow-derived mesenchymal stem cells in a photopolymerizing hydrogel. *Tissue Eng.* **2003**, *9*, 679−688.

(41) Huebsch, N.; Lippens, E.; Lee, K.; Mehta, M.; Koshy, S. T.; Darnell, M. C.; Desai, R. M.; Madl, C. M.; Xu, M.; Zhao, X.; Chaudhuri, O.; Verbeke, C.; Kim, W. S.; Alim, K.; Mammoto, A.; Ingber, D. E.; Duda, G. N.; Mooney, D. J. Matrix elasticity of void-forming hydrogels controls transplanted-stem-cell-mediated bone formation. *Nat. Mater.* **2015**, *14*, 1269−1277.

(42) Hadjipanayi, E.; Cheema, U.; Hopfner, U.; Bauer, A.; Machens, H. G.; Schilling, A. F. Injectable system for spatio-temporally controlled delivery of hypoxia-induced angiogenic signalling. *J. Controlled Release* **2012**, *161*, 852−860.

(43) Singelyn, J. M.; Christman, K. L. Injectable materials for the treatment of myocardial infarction and heart failure: the promise of decellularized matrices. *J. Cardiovasc. Transl. Res.* **2010**, *3*, 478−486.

(44) Carnicer-Lombarte, A.; Chen, S. T.; Malliaras, G. G.; Barone, D. G. Foreign Body Reaction to Implanted Biomaterials and Its Impact in Nerve Neuroprosthetics. *Front. Bioeng. Biotechnol.* **2021**, *9*, No. 622524.

(45) Anderson, J. M.; Rodriguez, A.; Chang, D. T. Foreign body reaction to biomaterials. *Semin. Immunol* **2008**, *20*, 86−100.

(46) Trindade, R.; Albrektsson, T.; Tengvall, P.; Wennerberg, A. Foreign Body Reaction to Biomaterials: On Mechanisms for Buildup and Breakdown of Osseointegration. *Clin. Implant Dent. Relat Res.* **2016**, *18*, 192−203.

(47) Luttikhuizen, D. T.; Harmsen, M. C.; Van Luyn, M. J. Cellular and molecular dynamics in the foreign body reaction. *Tissue Eng.* **2006**, *12*, 1955−1970.

(48) Wynn, T. A.; Vannella, K. M. Macrophages in Tissue Repair, Regeneration, and Fibrosis. *Immunity* **2016**, *44*, 450−462.

(49) Wynn, T. A.; Barron, L. Macrophages: master regulators of inflammation and fibrosis. *Semin. Liver Dis.* **2010**, *30*, 245−257.

(50) Martinez, F. O.; Gordon, S. The M1 and M2 paradigm of macrophage activation: time for reassessment. *F1000Prime Rep.* **2014**, *6*, 13.

(51) Wynn, T. A.; Chawla, A.; Pollard, J. W. Macrophage biology in development, homeostasis and disease. *Nature* **2013**, *496*, 445−455.

(52) Gretzer, C.; Emanuelsson, L.; Liljensten, E.; Thomsen, P. The inflammatory cell influx and cytokines changes during transition from acute inflammation to fibrous repair around implanted materials. *J. Biomater. Sci. Polym. Ed.* **2006**, *17*, 669−687.

(53) Heaney, R. *Principles of Bone Biology*; Academic Press: San Diego, 2008; Vol. 2.

(54) Maes, C.; Kobayashi, T.; Selig, M. K.; Torrekens, S.; Roth, S. I.; Mackem, S.; Carmeliet, G.; Kronenberg, H. M. Osteoblast precursors, but not mature osteoblasts, move into developing and fractured bones along with invading blood vessels. *Dev. Cell* **2010**, *19*, 329−344.

(55) Ben Shoham, A.; Rot, C.; Stern, T.; Krief, S.; Akiva, A.; Dadosh, T.; Sabany, H.; Lu, Y.; Kadler, K. E.; Zelzer, E. Deposition of collagen type I onto skeletal endothelium reveals a new role for blood vessels in regulating bone morphology. *Development* **2016**, *33*, 3933−3943.

(56) Kronenberg, H. M. Developmental regulation of the growth plate. *Nature* **2003**, *423*, 332−336.

(57) Einhorn, T. A.; Gerstenfeld, L. C. Fracture healing: mechanisms and interventions. *Nat. Rev. Rheumatol.* **2015**, *11*, 45−54.